http://dx.doi.org/10.5012/bkcs.2013.34.11.3261

Antibacterial Activity of CNT-Ag and GO-Ag Nanocomposites Against Gram-negative and Gram-positive Bacteria

Hyosuk Yun, Ji Dang Kim, Hyun Chul Choi,* and Chul Won Lee*

Department of Chemistry, Chonnam National University, Gwangju 500-757, Korea
**E-mail: chc12@chonnam.ac.kr (H. C. Choi); cwlee@jmu.ac.kr (C. W. Lee)*
Received July 4, 2013, Accepted August 9, 2013

Carbon nanocomposites composed of carbon nanostructures and metal nanoparticles have become one of useful materials for various applications. Here we present the preparation and antibacterial activity of CNT-Ag and GO-Ag nanocomposites. Their physical properties were characterized by TEM, XPS, and Raman measurements, revealing that size-similar and quasi-spherical Ag nanoparticles were anchored to the surface of the CNT and GO. The antibacterial activities of CNT-Ag and GO-Ag were investigated using the growth curve method and minimal inhibitory concentrations against Gram-negative and Gram-positive bacteria. The antibacterial activities of the carbon nanocomposites were slightly different against Gram-positive and Gram-negative bacteria. The proposed mechanism was discussed.

Key Words : Carbon nanostructures, Ag nanoparticles, Antibacterial activity, Gram-negative, Gram-positive

Introduction

Antibiotic resistance is a serious and growing phenomenon in public health and a big task in the field of pharmaceutical and medicine. Resistant pathogenic strains are emerging at a rate that far exceeds the speed of new antibiotic development. Therefore, the novel class of antibiotics having different mechanism of action in comparison to existing antibiotics is urgently needed. In the research area of antibiotics, development or searching of the antimicrobial compounds having improved or distinct antibacterial activity against multidrug-resistant (MDR) human pathogenic microbes is a primary intention.[1]

Nanotechnology has become an essential tool to develop the important properties of metal in the form of nanoparticles utilized for medical applications including diagnostics, drug delivery, biomarkers, and distinct antibacterial materials. In particular, silver nanoparticles (AgNPs) have been emerged as antimicrobial agents due to their high surface area to volume ratio and the unique physiochemical properties. Although the antibacterial mechanism of AgNPs is not fully understood, currently the great parts of the applications of AgNPs are in antibacterial and antifungal agents.[2,3] In spite of their high antibacterial activity, AgNPs is highly reactive and easily susceptible to aggregation into large particles due to their high surface energy of AgNPs, resulting in deterioration of their unique chemical properties and a loss of their antibacterial activities. Therefore many researchers have extensively studied various stable nanocomposites composed of AgNPs dispersed on suitable substrates.[4-7]

Carbon nanotube (CNT) and graphene oxide (GO) nanostructure possess outstanding properties and unique chemical architectures, which may serve as additive materials for the support of various metal nanoparticles. Recently several studies on the preparation, characterization, and antibacterial activities of carbon nanostructures combined with Ag nanoparticles have been reported.[8-12] While the carbon nanocomposites are a promising alternative to overcome a variety of problems resulting from the nanoparticle itself, still there are some difficulties in preparation of suitable nanocomposites. Antibacterial activities of silver nanocomposites depend on the size, shape and the degree of dispersion of AgNPs on the carbon nanostructures. We recently reported a simple and effective method for preparation of metal-supported carbon materials using thiolated carbon nanostructures, the samples observed in our experimentation having exhibited excellent catalytic activity in various organic and electrochemical reactions.[13-16] In this study, we present the preparation and characterization of CNT-Ag and GO-Ag nanocomposites using deposition of Ag nanoparticles on a thiolated CNT and GO surfaces. In addition, we tested the antibacterial activity against both Gram-negative and Gram-positive bacteria.

Experimental

Chemicals. Multiwall carbon nanotubes (MWNTs) were obtained from Carbon Nano Tech. Co., Ltd. (South Korea). Graphite powder (< 20 μm), potassium persulfate ($K_2S_2O_8$, 99.99%), phosphorus pentoxide (P_2O_5, 99.99%), potassium permanganate ($KMnO_4$, 99%), and silver nitrate ($AgNO_3$, 99%) were purchased from Sigma-Aldrich. Other reagents were of analytical grade and were used as received without further purification. All aqueous solutions were prepared with Milli-Q water (> 18.2 MΩ·cm) using the Direct Q3 system (Millipore).

Preparation of CNT-Ag. The MWNTs were stirred in an acid solution of HNO_3 and H_2SO_4 (1:3 by volume) at 90 ºC for 3 h. They were then filtered, washed with distilled water

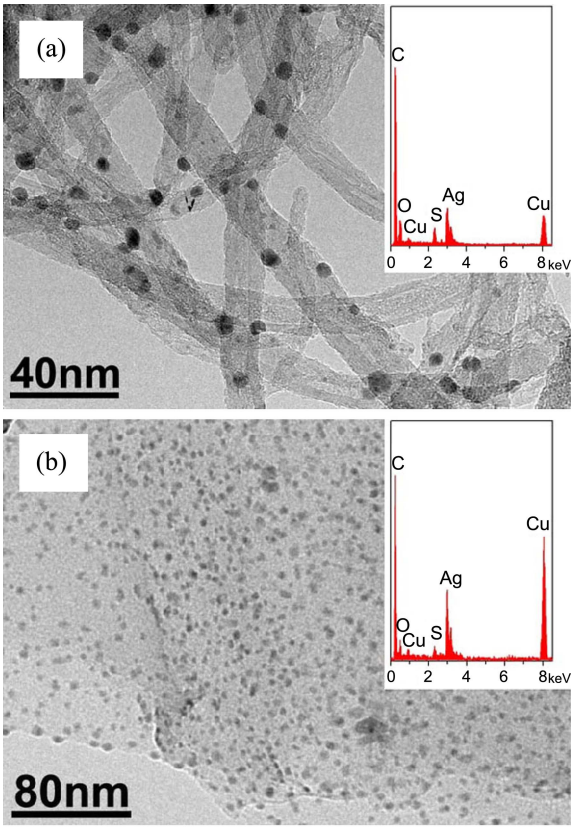

Figure 1. (a) TEM image of CNT-Ag CNT with its corresponding EDS spectrum (inset). (b) TEM image of the GO-Ag CNT with its corresponding EDS spectrum (inset).

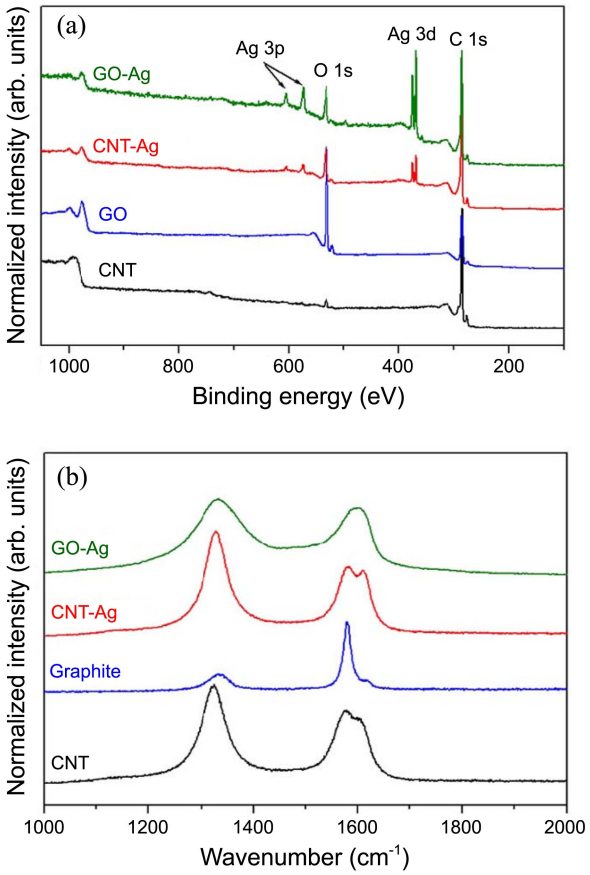

Figure 2. (a) XPS survey spectra of pristine CNT, pristine GO, CNT-Ag, and GO-Ag. (b) Raman spectra of pristine CNT, graphite, CNT-Ag, and GO-Ag.

(DI), and dried in an oven at 110 °C. To produce the thiol group, the acid-treated MWNTs were dispersed in THF, to which NaSH aqueous solution was added, and stirred at 50 °C for 12 h. The thiolation was confirmed by the XPS spectrum in the sulfur 2p region. Finally, the thiolated MWNTs (0.5 g) were dispersed in DI (15 mL), to which a 0.15 M $AgNO_3$ solution (20 mL) was added under stirring. Subsequently, a 0.1 M NaOH solution was added and stirred for 20 h. The CNT-Ag product was obtained by centrifugation, washed with DI water, and then vacuum dried at 40 °C for 24 h.

Preparation of GO-Ag. GO was prepared from graphite powder by the modified Hummers method.[17] The obtained GO (0.5 g) and DI water (30 mL) were added to a bottle (250 mL) and ultrasonicated for 20 min. Next, NaSH (8 g) was added gradually with stirring, and the mixture was then ultrasonicated for 1 h at 40 °C. The resultant mixture was maintained under stirring for 20 h at 55 °C to produce thiol groups on the GO surfaces. The product was filtered and washed with DI water and dried under vacuum at 50 °C for 3 h. The thiolated GO powder (0.1 g) was dispersed in DI water (30 mL) by sonication for 30 min. A 0.1 M $AgNO_3$ solution (0.5 mL) was then added to the GOSH solution under stirring. Subsequently, a 0.1 M NaOH solution was added under 20 h stirring. The GO-Ag product finally was obtained by centrifugation, washed with DI water, and then vacuum dried at 40 °C overnight.

Characterization of CNT-Ag and GO-Ag. TEM images were obtained using a JEM-2200FS microscope operated at 200 kV. Samples for the TEM analysis were prepared on a gold grid by dip-coating in dilute solutions. The XPS measurements were performed at the 4D beam line of the Pohang Light Source (PLS). For analysis of the XPS peaks, the C 1s peak position was set as 284.5 eV and used as the internal reference for location of the other peaks. Raman spectra were obtained at 633 nm using a Jobin Yvon/HORIBA LabRam ARAMIS Raman spectrometer equipped with an integral BX 41 confocal microscope.

Growth Curves of Bacterial Cells Exposed to Silver Nanoparticles. To determine the growth curves of Gram-negative and Gram-positive cells exposed to Ag colloid. The bacterial cell concentration was adjusted to 4×10^8 CFU/mL and incubated in a shaking incubator up to 6 h at 37 °C. Growth curves of bacterial cell cultures were attained through measures of the optical density at 600 nm.

Minimal Inhibitory Concentration (MIC) Measurements. The antibacterial activities of the silver nanocomposites were tested in sterile 96-well 200 mL plates as follows. Aliquots (100 mL) of the cell suspension at 4×10^6 CFU/mL in 1% peptone were added to 100 mL of the sample solutions (serial two-fold dilutions in 1% peptone). After

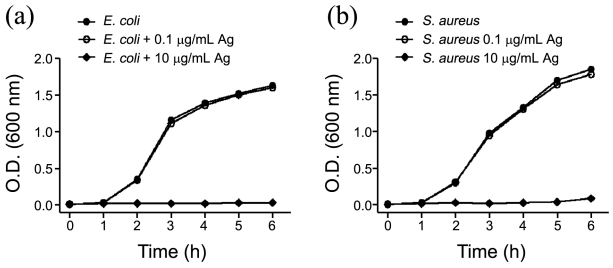

Figure 3. Growth curves of *E. coli* (a) and *S. aureus* (b) cells treated with different concentrations of silver nanoparticles.

incubation for 20 h at 37 °C, the MIC was determined by visual examinations on the basis of the lowest concentration of sample solution in cells with no bacterial growth. Two types of Gram-positive bacteria (*Bacillus subtilis* [KCTC 3068] and *S. aureus* [KCTC 1621]) and two types of Gram-negative bacteria (*Escherichia coli* [KCTC 1682] and *Salmonella typhimurium* [KCTC 1926]) were procured from the Korean Collection for Type Cultures (KCTC) at the Korea Research Institute of Bioscience and Biotechnology.

Field Emission Scanning Electron Microscopy (FE-SEM). To directly observe the morphological changes of the bacterial cells after CNT-Ag treatment, FE-SEM was employed. Bacterial cells (4×10^6 CFU/mL) were treated with 10 mg/mL of CNT-Ag for 3 h, and washed with phosphate buffered saline (PBS) 3 times and pre-fixed with 2% glutaraldehyde and 2% paraformaldehyde for 4 h. The pre-fixed cells were washed with 0.05 M cacodylate buffer three times and post-fixed with 1% osmium tetroxide for 1 h. After washing with 0.05 M cacodylated buffer, dehydration process was conducted with 30, 50, 70, 90, 95, and 100% of ethanol. The fixed cell was dried and gold-coated using ion sputter. The pre-treated samples were observed by FE-SEM (JSM-7500F, JEOL, Japan).

Results and Discussion

Preparation and Characterization of CNT-Ag and GO-Ag. Figures 1(a) and (b) show typical TEM images of CNT-Ag and GO-Ag, which show clearly the presence of a large number of nanoparticles anchored to the surfaces of both samples. The adhered nanoparticles in the quasi-spherical morphology are uniformly dispersed on the surfaces of the CNT-Ag and GO-Ag. For both samples, most of the nanoparticle diameters ranged from 2 to 4 nm. The corresponding energy-dispersive X-ray (EDS) analysis showed that the species supported on the CNT-Ag and GO-Ag was Ag [Figs. 1(a) and (b), insets]. Figure 2(a) shows a series of XPS survey spectra from the pristine CNT, pristine GO, CNT-Ag and GO-Ag. For the pristine CNT and GO, the XPS data shows distinct C and O 1s peaks and no other elements are detected. However, after Ag deposition, the presence of Ag element is detected from the both samples. The relative surface atomic ratio was estimated from the corresponding peak areas, corrected with the tabulated sensitivity factors. The estimated value of the Ag content is 3.4 and 6.4 atomic %, respectively, for CNT-Ag and GO-Ag. Raman spectroscopy was used to obtain information on the average crystallinities of CNT-Ag and GO-Ag. As shown in Figure 2(b), the spectrum consisted of two bands at ~1330 cm^{-1} (D band) and 1570 cm^{-1} (G band). The integrated intensity ratio of the D band to the G band (I_D/I_G) had a linear relation to the inverse of the in-plane crystallite dimension. The I_D/I_G values were approximately 1.42, 0.21, 1.70, and 1.12 for the pristine CNT, graphite, CNT-Ag, and GO-Ag, respectively.

Table 1. Summary of minimal inhibitory concentration (mg/mL) against Gram-negative and Gram-positive bacteria

		Ag colloid	CNT-Ag	GO-Ag	GO-Ag(I)[a]
Gram (–)	*E. coli*	0.21	0.13	0.5	4
	Salmonella	0.21	0.25	0.25	4
Gram (+)	*B. subtilis*	1.69	0.5	4	16
	S. aureus	3.37	1	4	8

[a]Treated with H_2O_2

Antibacterial Activity of Silver Nanocomposites. The antibacterial activities of silver nanocomposites were investigated by determining bacterial growth rate and minimal inhibitory concentration with a Gram-negative bacterium *E. coli* and a Gram-positive bacterium *S. aureus*. To measure the growth rate of bacteria, cells were cultured in LB broth with Ag colloid, CNT-Ag, and GO-Ag, and the results were determined by optical density (OD) measurements at 600 nm. However, since CNT and GO displayed very high optical density at 600 nm, we obtained reliable growth curves with only Ag colloid and shown in Figure 3. With 10 mg/mL concentration, Ag colloid completely inhibited bacteria cell growth of both Gram-negative *E. coli* and Gram-positive *S. aureus*, but there were no effects with 0.1 mg/mL concentration of Ag colloid. In order to obtain more comprehensive antibacterial activities of the nanocomposites and the lowest concentration that completely inhibit cell growth, we measured the minimal inhibitory concentration (MIC) of the nanocomposites against two different species of Gram-negative and Gram-positive bacteria (Table 1). The results clearly indicate that the MIC values of Gram-negative bacteria were lower than those of Gram-positive bacteria for Ag colloid, CNT-Ag and GO-Ag nanocomposites. These data may result from the distinct structure of cell wall between Gram-negative and Gram-positive bacteria. The cell wall of Gram-negative bacteria is composed of thin peptidoglycan layer (7-8 nm) with additional an outer membrane. In contrast, Gram-positive bacteria contain a thick peptidoglycan layer (20-80 nm) in the outside the cell wall without an outer membrane. Peptidoglycan is a mesh-like polymer consisting of sugars and amino acids. The thick peptidoglycan of Gram-positive bacteria may also include other components such as teichoic and lipoteichoic acids and complex polysaccharides, which serve to act as chelating agents and also for certain types of adherence. Therefore, peptidoglycan layer protects against antibacterial agents such as antibiotics, toxins, chemical, and degradative enzymes.

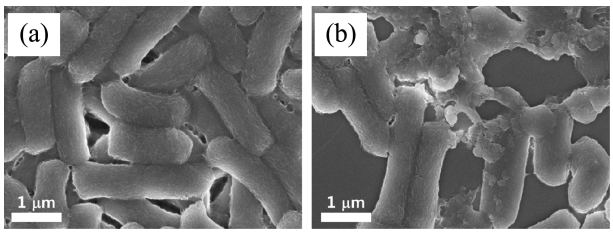

Figure 4. FE-SEM micrograph of *E. coli* before (a) and after (b) exposure to CNT-Ag nanocomposites.

In present study, the antibacterial activities of the silver nanocomposites were lower against Gram-positive bacteria than Gram-negative bacteria. Several previous reports also showed that Gram-positive bacteria have slightly higher resistance to silver antibacterial agents than Gram-negative bacteria.[18,19] The MIC value of CNT-Ag was lower than those of other silver nanocomposites against both Gram-negative and Gram-positive bacteria with an exception for *Salmonella*, which showed similar effects to all nanocomposites. High antibacterial activity of CNT-Ag may result from the good dispersion of the Ag nanoparticles on the CNT and great water-dispersion property compared to GO nanostructure. Morphological changes of *E. coli* cells by CNT-Ag were studied using FE-SEM (Fig. 4). The untreated cells of were typically rod-shaped and the cell surface was intact (Fig. 4(a)). However, in CNT-Ag treated cells, severe fragmentations were observed (Fig. 4(b)). The mechanisms of antibacterial activities of Ag nanoparticles have been partially known. Ag nanoparticles may attack the bacterial membrane, leading to changing of the permeability of the membranes, leakage of reducing sugars and proteins and inactivation of the respiratory chain dehydrogenases.[18,19] Ag nanoparticles also induce pits and gaps in the bacterial membrane and the cell membrane was fragmentary.[20] Several researchers suggested that free-radicals or Ag ions produced by Ag nanoparticles attack outer bacterial membrane or peptidoglycan layer and then induce irregular fragmentations of the bacterial cells.[21] We also verified the effect of oxidized Ag species on the antibacterial activity. GO-Ag(I) oxidized by H_2O_2 contains around 50% Ag(I) on the surface of Ag nanoparticles attached to GO.[13] Interestingly, the antibacterial activity of GO-Ag(I) was reduced up to 16-folds compared to GO-Ag by the MIC test (Table 1). One possible mechanism is that the productions of free-radicals or Ag ions by GO-Ag(I) are reduced by oxidation of Ag and then decrease the antibacterial activity.

Conclusion

We have introduced Ag nanoparticles on to CNTs and GOs by surface thiolation. These synthetic CNT-Ag and GO-Ag showed slightly higher antibacterial activities against Gram-negative than Gram-positive bacteria. The antibacterial activity of CNT-Ag was the highest in both Gram-negative and positive bacteria, suggesting that CNT-Ag is a promising antibacterial agent for broad range of antibiotics.

Acknowledgments. This study was financially supported by Chonnam National University, 2011. Experiments at PLS were supported in part by MSIP and POSTECH.

References

1. Lara, H. H.; Ayala-Nunez, N. V.; Turrent, L. D. I.; Padilla, C. R. *World J. Microb. Biot.* **2010**, *26*, 615.
2. Seil, J. T.; Webster, T. J. *Int. J. Nanomedicine* **2012**, *7*, 2767.
3. Rai, M. K.; Deshmukh, S. D.; Ingle, A. P.; Gade, A. K. *J. Appl. Microbiol.* **2012**, *112*, 841.
4. Roy, B.; Bharali, P.; Konwar, B. K.; Karak, N. *Bioresource Technology* **2013**, *127*, 175.
5. Angelova, T.; Rangelova, N.; Yuryev, R.; Georgieva, N.; Muller, R. *Mat. Sci. Eng. C-Mater.* **2012**, *32*, 1241.
6. Cao, X. L.; Tang, M.; Liu, F.; Nie, Y. Y.; Zhao, C. S. *Colloid. Surface B* **2010**, *81*, 555.
7. Zhang, Y.; Zhong, S. L.; Zhang, M. S.; Lin, Y. C. *J. of Mater. Sci.* **2009**, *44*, 457.
8. Tai, Z. X.; Ma, H. B.; Liu, B.; Yan, X. B.; Xue, Q. J. *Colloid. Surface B* **2012**, *89*, 147.
9. Liu, X.; Yu, L. M.; Liu, F.; Sheng, L. M.; An, K.; Chen, H. X.; Zhao, X. L. *J. Mater. Sci.* **2012**, *47*, 6086.
10. Ma, J. Z.; Zhang, J. T.; Xiong, Z. G.; Yong, Y.; Zhao, X. S. *J. Mater. Chem.* **2011**, *21*, 3350.
11. Li, Z. Z.; Fan, L. J.; Zhang, T.; Li, K. *J. Hazard Mater.* **2011**, *187*, 466.
12. Das, M. R.; Sarma, R. K.; Saikia, R.; Kale, V. S.; Shelke, M. V.; Sengupta, P. *Colloid. Surface. B* **2011**, *83*, 16.
13. Kim, J. D.; Palani, T.; Kumar, M. R.; Lee, S. W.; Choi, H. C. *J. Mater. Chem.* **2012**, *22*, 20665.
14. Jeong, Y. N.; Choi, M. Y.; Choi, H. C. *Electrochim. Acta* **2012**, *60*, 78.
15. Kim, J. Y.; Park, K.; Bae, S. Y.; Kim, G. C.; Lee, S.; Choi, H. C. *J. Mater. Chem.* **2011**, *21*, 5999.
16. Kim, J. Y.; Jo, Y.; Lee, S.; Choi, H. C. *Tetrahedron Lett.* **2009**, *50*, 6290.
17. Kovtyukhova, N. I.; Ollivier, P. J.; Martin, B. R.; Mallouk, T. E.; Chizhik, S. A.; Buzaneva, E. V.; Gorchinskiy, A. D. *Chem. Mater.* **1999**, *11*, 771.
18. Jung, W. K.; Koo, H. C.; Kim, K. W.; Shin, S.; Kim, S. H.; Park, Y. H. *Appl. Environ. Microb.* **2008**, *74*, 2171.
19. Feng, Q. L.; Wu, J.; Chen, G. Q.; Cui, F. Z.; Kim, T. N.; Kim, J. O. *J. Biomed. Mater. Res.* **2000**, *52*, 662.
20. Amro, N. A.; Kotra, L. P.; Wadu-Mesthrige, K.; Bulychev, A.; Mobashery, S.; Liu, G. Y. *Langmuir* **2000**, *16*, 2789.
21. Pellieux, C.; Dewilde, A.; Pierlot, C.; Aubry, J. M. *Method Enzymol.* **2000**, *319*, 197.